1981

Collisional depolarization of state selected (J,M J) BaO A 1Σ+ measured by optical–optical double resonance

Stuart J. Silvers
Virginia Commonwealth University

Richard A. Gottscho
Massachusetts Institute of Technology

Robert W. Field
Massachusetts Institute of Technology

Silvers, S. J., Gottscho, R. A., & Field, R. W. Collisional depolarization of state selected (J,M J) BaO A 1Σ+ measured by optical–optical double resonance. The Journal of Chemical Physics, 74, 6000 (1981).

Collisional depolarization of state selected (J,M_J) BaO $A\ ^1\Sigma^+$ measured by optical–optical double resonance

Stuart J. Silvers

Department of Chemistry, Virginia Commonwealth University, Richmond, Virginia 23284

Richard A. Gottscho[a),b)] and Robert W. Field

Department of Chemistry, Massachusetts Institute of Technology, Cambridge, Massachusetts 02139
(Received 16 September 1980; accepted 21 November 1980)

The optical–optical double resonance (OODR) technique is used to investigate the change in magnetic quantum number (M) a state selected molecule undergoes on collision with other molecules. A first linearly polarized dye laser prepares $A\ ^1\Sigma^+$BaO($v=1$) in the $J=1$, $M=0$ sublevel. The extent of collisional transfer to other M sublevels of both $J=1$ and $J=2$ is then probed by a second polarized dye laser which induces fluorescence from the $C\ ^1\Sigma^+$ state. Elastic collisions ($\Delta J=0$) between BaO ($A\ ^1\Sigma^+$) and CO_2 are observed to change M from 0 to ± 1 leaving J unchanged. The total elastic M-changing cross section is $\sigma^{\Delta M}_{CO_2}=8.4\pm2.4$ Å^2. Inelastic collisions ($\Delta J=+1$) which transfers molecules to $J=2$ also cause M changes, with both Ar and CO_2 as collision partners. M, the *space-fixed* projection of J, is found to be neither conserved nor randomized. Quantum atom–diatom collision models with quantization axis along the relative velocity vector are considered. Transition amplitudes in this system are evaluated using the l-dominant and CS approximations.

I. INTRODUCTION

The manner in which collisions change M quantum numbers and reorient molecules can be investigated in simple, well-defined systems when high resolution, tunable lasers are used. The optical–optical double resonance technique (OODR)[1] is used here for such investigations. A first (pump) laser prepares as few as one M sublevel of a particular rovibrational state. Other sublevels are then populated by elastic ($\Delta J=0$) and inelastic ($\Delta J\neq 0$) collisions. The altered populations are sampled by a second tunable (probe) laser which induces transitions to a higher electronic state from which fluorescence is detected. For elastic collisions, M sublevel populations are directly obtained. For inelastic collisions, OODR intensity as a function of probe polarization is compared to the predictions from various models of M-changing collisions to determine which, if any, is applicable.

Five other techniques have been utilized to measure collision induced molecular depolarization: (i) resonance fluorescence[2–4]; (ii) microwave and infrared double resonance[5–8]; (iii) Hanle effect experiments[9–11]; (iv) laser induced line narrowing[12]; and (v) molecular beam electric resonance experiments.[13] The results of these experiments differ widely, depending upon the particular molecular system chosen for investigation.

For homonuclear atom–diatom collisions, the results have been somewhat inconsistent primarily because of experimental difficulties. Kurzel and Steinfeld[3] reported final J averaged, inelastic depolarization cross sections of 5 to 20 Å^2 for I_2^* colliding with H_2, He, or Ne. These cross sections correspond to average J reorientation angles, referred to a laboratory reference frame, of 43° to 50°.[3] Lack of final state selection, excitation of more than one initial level, and multiple collision effects obscure the meaning of these measurements. McCaffery *et al.*[4(a),4(b)] concluded from higher resolution experiments that in fact the space fixed magnetic quantum number M, is *conserved* in collisions between I_2^* and O_2, I_2, or Ar.[14] Unfortunately, McCaffery *et al.*'s measurements were also flawed by preparation of more than one initial J level and by the effects of multiple collisions.[4(a),4(b)]

In another series of resonance fluorescence experiments, McCaffery *et al.*[4(c),(d)] concluded that there are restricted channels by which rotational energy is transferred in Li_2^* ~ He collisions; they found that the propensity rule $\Delta M\leq\Delta J$ is valid. These measurements were not subject to the problems encountered in the I_2^* experiments, but it now remains to determine the generality of this conclusion. For elastic collisions, for example, little depolarization would be expected; but only inelastic events were examined.[4] Is this propensity rule valid for polar diatoms or affected by collision partner polarizability?

Borkenhagen *et al.*[13] have measured both elastic and inelastic M changes in CsF, induced by collisions with the rare gases He through Ar, using the molecular beam-electric resonance method. Their results are most interesting in light of the similarity between their experimental system and ours, although we utilize no molecular beams. Their experiments involve only the lowest rotational levels of CsF ($X\ ^1\Sigma^+$), $J=1$ to 3 and M changes of 0 or 1. We examine the $J=1$ and 2 levels of BaO ($A\ ^1\Sigma^+$) and M changes of 0, ±1, and ±2. Although the molecules are isoelectronic, the BaO ($A\ ^1\Sigma^+$) dipole moment, 2.20 D,[15] is 3.6 times smaller than the CsF dipole moment, 7.89 D.[16] For $(J,M)=(1,1)\rightarrow(1,0)$ collisions, Borkenhagen *et al.* measured cross sections of 5 Å^2 for Ne, Ar, and Kr. For $\Delta J=1$ (e.g., $1\rightarrow2$), comparable cross sections were determined for both $\Delta M=0$ and 1. No systematic variation with rare gas was evident.[13] Our results on BaO ~ Ar provide a unique op-

[a)]Present address: Bell Laboratories, Murray Hill, New Jersey 07974.

[b)]Chaim S. Weizmann postdoctoral fellow.

 0021-9606/81/116000-09$01.00

portunity to assess the importance of the diatom dipole and quadrupole moments on M changing collisions.

Additional experiments on polyatomic polar systems have suggested that low J, K levels are easily depolarized whereas high J, K levels are not.[6] Shoemaker *et al.* reported a cross section of ≈ 100 Å^2 for $\Delta J = 0$, $\Delta M = \pm 1$ $CH_3F \sim CH_3F$ collisions, but this value is only an estimate as it represents an average over the upper $(J, K) = (5, 3)$ and lower $(J, K) = (4, 3)$ rovibrational levels. For higher J, K values, no depolarization was detected, indicating that the cross sections were at least 100 times smaller.[6] In addition to the upper/lower level ambiguity, these measurements were also imprecise owing to spectral overlap.[6]

The experiments described here simplify interpretation by preparing BaO $(A\,^1\Sigma^+)$ $(v = 1)$ in the single $J = 1$, $M = 0$ sublevel. The sub-Doppler resolution of the OODR technique eliminates the problem of overlapping transitions near the band origin, permitting preparation of this unique level.

The M sublevel populations of $J = 1$ are probed by tuning the second laser to the $P(1)$ line of the $C \leftarrow A$ 3-1 band. With the probe polarization perpendicular to that of the pump laser, the upper C state $(J^* = 0)$ cannot be excited from the initially prepared $M = 0$ sublevel. *An OODR signal does not appear unless collisions change M.* In this on-off type experiment, *any* fluorescence signal is *direct* evidence for elastic transfer to $M = \pm 1$ from $M = 0$. Such transfer is detected in collisions with CO_2 *but not with Ar*, in contrast with $CsF \sim Ar$ results mentioned above. The CO_2 elastic transfer cross section is comparable in size to that for level to level $(J \rightarrow J')$ transfer.[1(a)]

When the probe laser is tuned to the $P(2)$ line, information is obtained on the manner in which collisions transfer molecules from $J = 1$, $M = 0$ into M sublevels of $J = 2$. The extent of $J = 2$ polarization is characterized and significant population in $M \neq 0$ sublevels is detected. Different models for inelastic depolarization are then considered in an attempt to distinguish the one(s) best able to account for observations. In this inelastic case, we find that Ar and CO_2 produce comparable effects.

II. EXPERIMENTAL

The oven for generating BaO has been described elsewhere.[17] Ba metal (Alfa 99.999% purity) is heated to melting and the Ba atoms are entrained by Ar (Airco, 99.998% purity) and mixed with CO_2 (Airco, 99.8% purity) to form BaO according to the reaction

$$Ar + Ba + CO_2 \rightarrow BaO + CO + Ar\ .$$

The operating pressures of the reactants are in the range 0.24–4.4 Torr Ar, 0.01–0.30 Torr CO_2, and 1×10^{-4} Torr Ba. CO_2 and Ar pressures are measured by Wallace and Tiernan Model FA160 and MKS Baratron Model 220-2A6-1 gauges.

The dye lasers (Coherent CR 599-21) operate in single mode at typically 50 mW output power. They are frequency stabilized with 1 MHz linewidths. The optics, frequency calibration, and fluorescence detection are

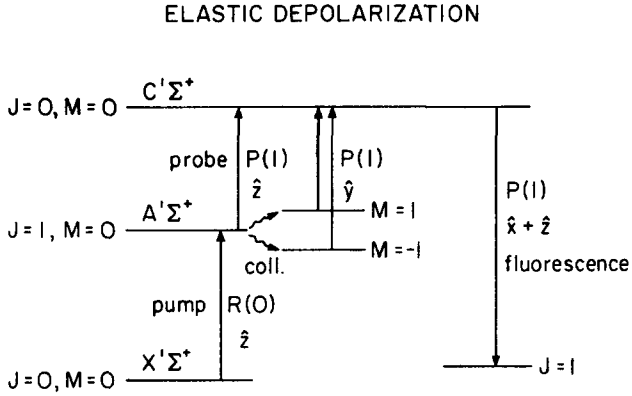

FIG. 1. Elastic depolarization experiment.

essentially the same as described previously.[1] The pump laser beam is $\hat{z}$ polarized with a calcite polarizer and propagates in the $\hat{x}$ direction. The probe laser radiation is first circularly polarized by a Fresnel rhomb and is then linearly polarized (with a 50% loss) in either the $\hat{y}$ or $\hat{z}$ directions by a second rotatable calcite polarizer; it propagates collinearly with the pump beam.

A. The elastic depolarization experiment

The $\hat{z}$ polarized pump laser is tuned to the $R(0)$ line of the $A\,^1\Sigma^+$ $(v = 1) \leftarrow X\,^1\Sigma^+$ $(v'' = 0)$ band, preparing the $|J = 1, M = 0\rangle$ sublevel. The probe laser is then tuned to the $P(1)$ line of the $C\,^1\Sigma^+$ $(v^* = 3) \leftarrow A\,^1\Sigma^+$ $(v = 1)$ band. When the probe laser is $\hat{z}$ polarized, the $\Delta M = 0$ selection rule applies and the intensity of fluorescence from $C\,^1\Sigma^+$ depends only on the $M = 0$ population. When the probe polarization is rotated to $\hat{y}$, $\Delta M = \pm 1$ applies and fluorescence from the $C\,^1\Sigma^+$ state is *only* detected if *collisions* have populated the $M = \pm 1$ sublevels. Any OODR signal is direct evidence for elastic M-changing collisions.[18] The scheme of this experiment is shown in Fig. 1.

Ultraviolet $C\,^1\Sigma^+ \rightarrow X\,^1\Sigma^+$ fluorescence in the $\hat{y}$ direction is detected with a photomultiplier (Hamamatsu R212 at -600 V dc). The probe laser scans through the $P(1)$ transition and integrated intensities are measured. The ratio of the intensity when pump and probe polarizations are perpendicular $(I_\perp)$ to that when they are parallel $(I_\parallel)$ is a measure of the extent of population transfer to the $M = \pm 1$ levels. This ratio $(I_\perp/I_\parallel)$ is small and care must be taken to correct for any laser depolarization occurring before the beams enter the vacuum chamber. Laser depolarization results in unwanted $I_\parallel$ intensity when the lasers are in the perpendicular configuration. Correction is made by introducing a calcite analyzer at the place both beams enter the chamber. Any OODR excited UV fluorescence intensity when the analyzer is set in the $\hat{y}$ or $\hat{z}$ directions is due to laser depolarization by mirrors and beam-splitters, not to collisional effects. The probe laser has different intensities when $\hat{z}$ and $\hat{y}$ are polarized, and this too is corrected for.

B. The inelastic depolarization experiment

The pump laser again prepares $|J = 1, M = 0\rangle$. The probe laser is now tuned to the $P(2)$ line so that M sub-

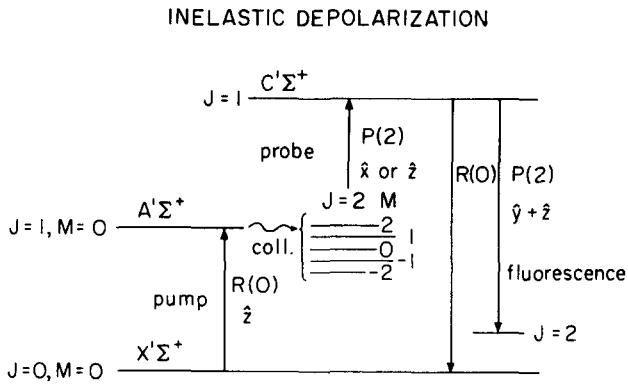

FIG. 2. Inelastic depolarization experiment.

level populations of $J=2$ can be probed. These populations are the result of inelastic transfer from $J=1$. When the laser polarizations are parallel ($\hat{z}$), the intensity of fluorescence from the $C\,^1\Sigma^+$ state depends on the sublevel populations in a way that differs from its dependence in the perpendicular configuration. The ratio of intensities in the two configurations is expressed in terms of the sublevel populations [Eq. (6) below] and is a measure of the extent of angular momentum realignment accompanying collisional transfer from $J=1$ to $J=2$. Figure 2 depicts this experiment.

III. RESULTS AND DISCUSSION

A. Elastic depolarization

The $J=1$ state prepared by the pump laser is characterized by a density matrix $\rho_{M'M}$ whose only nonvanishing matrix element is ρ_{00}. The density matrix may be decomposed into state multipoles $\langle T_{KQ}\rangle$.[19,20] If any moment with $K>0$ exists, the state is said to be *polarized*. If a dipole component $\langle T_{1Q}\rangle$ is present, the state is *oriented*. If a quadrupole component $\langle T_{2Q}\rangle$ exists, the state is *aligned*. Here the density matrix of the optically excited state has no dipole component but does have a nonvanishing quadrupole one, $\langle T_{20}\rangle$, and the prepared state is aligned; the detection of fluorescence with the beam polarizations perpendicular is then an indication that the prepared alignment has been changed by collisions.

The corrected $I_\perp/I_\parallel$ ratio is related to sublevel populations by starting with the general expression for fluorescence intensity in the absence of external fields when sublevels are degenerate[21]:

$$I \propto \sum_{m,m'} F^i_{mm'} G^f_{m'm} \,. \tag{1}$$

The excitation matrix is given by

$$F^i_{mm'} = \sum_{M,M'} \langle m|\hat{e}_i|M\rangle\langle M'|e_i|m'\rangle \rho_{MM'} \,, \tag{2}$$

where m and m' designate upper state (J^*) magnetic sublevels and M and M' lower state (J) ones.[22] The polarization vector for excitation is $\hat{e}_i$ and the elements of the lower state density matrix ρ are given by

$$\rho_{MM'} = \sum_{n=1}^{N} a_M^{(n)} a_{M'}^{(n)*} \,,$$

where $a_M^{(n)}$ is the amplitude for finding the nth molecule in the sublevel M and N is the total number of molecules. The diagonal elements are sublevel populations; the off-diagonal ones vanish unless definite phase relations, or coherences, exist between sublevel amplitudes. The emission matrix is given by

$$G^f_{m'm} = \sum_{\mu} \langle m'|\hat{e}_f|\mu\rangle\langle\mu|\hat{e}_f|m\rangle \,, \tag{3}$$

where $\hat{e}_f$ is the polarization vector for detection and μ designates ground state sublevels to which emission occurs.

In the elastic experiment, probe excitation and subsequent emission are both $P(1)$ transitions and Eq. (1) reduces to

$$I_\parallel \propto F^z_{00} G^{x+z}_{00} = F^z_{00}(G^x_{00} + G^z_{00}) \,,$$

$$I_\perp \propto F^y_{00} G^{x+z}_{00} \,.$$

Coherence is not optically prepared here and cannot be generated by the axially symmetric (about $\hat{z}$) collisional perturbations,[20] thus only diagonal elements of ρ need be included in Eq. (2). By symmetry, collisions will populate the $M=\pm1$ sublevels equally ($\rho_{11}=\rho_{-1-1}=n_1$). The necessary F and G elements are calculated using appropriate direction cosine matrix elements[23] and are listed in Table I. $I_\perp$ and $I_\parallel$ are then evaluated to obtain

$$I_\perp/I_\parallel = \rho_{11}/\rho_{00} = n_1/n_0 \,.$$

The intensities are directly proportional to the sublevel population densities, n_i.

The intensity ratio ($I_\perp/I_\parallel$) has been measured at different Ar and CO_2 pressures. At low CO_2 pressure, the ratio is less than 0.03 and does not vary noticeably with Ar pressure. Thus, an upper bound for elastic depolarization by Ar is $\sigma_{Ar} < 1$ Å^2. The finite value of $I_\perp$ at low CO_2 pressure (0.03 Torr) is due either to higher than indicated residual CO_2 pressure or incomplete correction for laser beam depolarization.

When the CO_2 pressure is varied, significant change in the population ratio is observed; this pressure dependence is shown in Fig. 3. Measurements at fixed Ar pressure of 0.3 Torr are shown by open circles. Averages of measurements at different Ar pressures but

TABLE I. Excitation and emission matrices.

	$F^{(x)}$	$F^{(z)}$
F_{00}	$\frac{1}{5}n_1$	$\frac{4}{15}n_0$
$F_{11}=F_{-1-1}$	$\frac{1}{30}n_0+\frac{1}{5}n_2$	$\frac{1}{5}n_1$
$F_{1-1}=F_{-11}$	$-\frac{1}{30}n_0$	0
	$G^{(y)}$	$G^{(z)}$
G_{00}	$\frac{1}{5}$	$\frac{9}{15}$
$G_{11}=G_{-1-1}$	$\frac{6}{15}$	$\frac{1}{5}$
$G_{1-1}=G_{-11}$	$\frac{3}{15}$	0

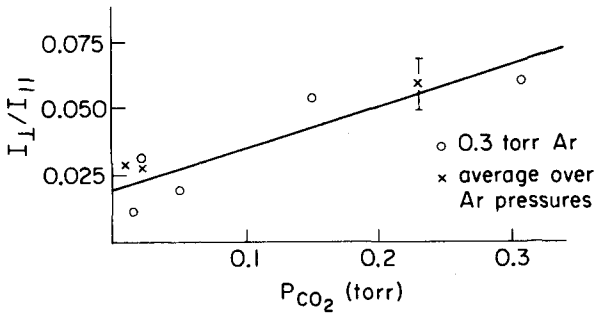

FIG. 3. Pressure dependence of the intensity ratio $I_\perp/I_\parallel$ for the elastic depolarization experiment.

constant CO_2 pressure are shown by crosses. The points are fit to a straight line whose slope is related as follows to the cross section $\sigma_{CO_2}^{\Delta M}$ for elastic M-changing collisions.

If an excited BaO molecule is assumed to undergo at most one collision,[24] the rate at which the $M=+1$ sublevel is populated is given by

$$dn_1/dt = k_{CO_2} n_0 n_{CO_2} + k_{Ar} n_0 n_{Ar} - k_{rad} n_1 \ , \tag{4}$$

where k_{CO_2} and k_{Ar} are the rate constants for transfer from $M=0$ to $+1$ through collisions with CO_2 and Ar, respectively. The rate at which the probe laser removes molecules is small compared to the radiative rate k_{rad} and is not included in Eq. (4). Since $I_\perp/I_\parallel$ is shown by experiment not to depend on P_{Ar}, k_{Ar} is neglected and a steady state solution obtained:

$$n_1/n_0 = I_\perp/I_\parallel = k_{CO_2} n_{CO_2}/k_{rad} \ . \tag{5}$$

Using 2.75×10^6 sec^{-1} for k_{rad}[25] and the slope from Fig. 3, the rate constant for changing M from 0 to $+1$ is k_{CO_2} $(J=1\to1, M=0\to+1) = 2.0\pm0.6\times10^{-11}$ cm^{3}sec^{-1}, and the corresponding cross section is $\sigma_{CO_2} = 4.2\pm1.2$ Å^2. Since the cross section for changing M to -1 will have the same value, the total cross section for elastic ΔM transfer is $\sigma_{CO_2}^{\Delta M} = 8.4\pm2.4$ Å^2. This is comparable in size to that for $J=0\to J_f=1$ transfer ~20 Å^2, which in turn accounts for ≈20% of the total inelastic cross section.[1(a)]

B. Inelastic depolarization

With the probe laser tuned to $C\,^1\Sigma^+ - A\,^1\Sigma^+$ 3-1 $P(2)$, the fluorescence intensities with the laser polarizations parallel and perpendicular are measured. These intensities can again be related to the M level populations of the state being probed ($J=2$). Excitation is from $J=2$ to $J^*=1$ and emission is to $J''=2$ and 0. From Eq. (1) the intensities are

$$I_\parallel \propto F_{00}^z G_{00}^{x+z} + 2F_{11}^z G_{11}^{x+z} \ ,$$

$$I_\perp \propto F_{00}^y G_{00}^{x+z} + 2F_{11}^y G_{11}^{x+z} + 2F_{1-1}^y G_{-11}^{x+z} \ .$$

Collisions cannot generate orientation or coherences in $J=2$[20] and

$$\rho_{MM'} = 0 \ , \quad M \neq M' \ , \quad \rho_{11} = \rho_{-1-1} = n_1 \ , \quad \rho_{22} = \rho_{-2-2} = n_2 \ .$$

The F and G matrices are then calculated (and given in Table I) to obtain

$$I_\perp/I_\parallel = (n_0 + 6n_1 + 9n_2)/(8n_0 + 9n_1) \ . \tag{6}$$

The intensity ratio is measured in a series of eleven experiments at different pressures. The argon pressure is varied between 0.3 and 2.7 Torr and the CO_2 pressure between 0.01 and 0.32 Torr. The variation of the intensity ratio with total pressure is shown in Fig. 4. The ratio apparently does not depend on whether CO_2

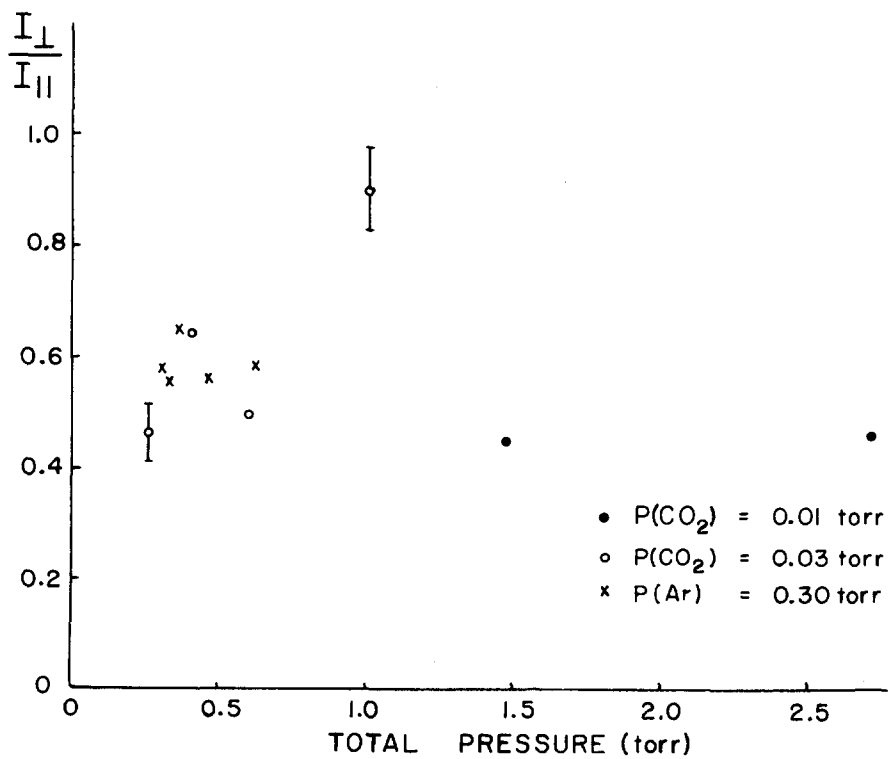

FIG. 4. Pressure dependence of the intensity ratio $I_\perp/I_\parallel$ for the inelastic depolarization experiment.

or Ar is the primary collision partner[26] and does not vary with total pressure. The average value of the intensity ratio is $I_\perp/I_\parallel = 0.58 \pm 0.05$ (1σ error).

At first thought, it is surprising that multiple collisions do not increase the intensity ratio as pressure is increased. However, a simple kinetic model predicts only a small change in the intensity ratio over the pressure range used. This model restricts transitions to levels with $J \leq 3$ and specifies $\Delta M \leq \Delta J$. The rate constants for allowed transitions are all taken equal (2×10^6 $\text{sec}^{-1}\,\text{Torr}^{-1}$). The pump rate into $|10\rangle$ is at least 10 times greater than the rate of collisional repopulation of this level. When this is done and steady state populations are calculated at different pressures, it is seen that the intensity ratio increases only by 0.08 over the experimental pressure range. An increase of this size is hidden by experimental error; we thus conclude that this experiment is insensitive to the effects of multiple collisions.

The observed intensity ratio immediately implies that levels other than $M=0$ of $J=2$ are significantly populated by collisions and that a $\Delta M = 0$ selection rule in the laboratory frame does not apply to this inelastic transfer. If such a selection rule did apply, the intensity ratio would be 0.125. Also ruled out is complete depolarization (M randomization), since this would result in a ratio of 0.94. We can conclude that the depolarization is significant but not complete.

Instead of the intensity ratio ($I_\perp/I_\parallel$), a degree of polarization (P) can be defined and used to characterize the population distribution among M sublevels of $J=2$:

$$P = (I_\parallel - I_\perp)/(I_\parallel + I_\perp)\ . \tag{7}$$

P has the advantage of increasing as the state's polarization increases. The observed value for P is 0.27. In the $\Delta M = 0$ and M randomization limiting cases, P values would be 0.78 and 0.03, respectively. In the following sections the phrase "intensity ratio" refers to $I_\perp/I_\parallel$, while "degree of polarization" refers to P.

Another means of visualizing inelastic M changing collisions is to lengthen and then rotate **J** out of the laboratory-fixed plane (xy), in which it is initially prepared. M sublevels are populated to an extent determined by the rotation angle. The angle which matches the observed intensity ratio of 0.58 is $\beta = 36°$.[27]

C. Models for M transfer

1. *Long-range intermolecular forces*

Several long range interactions may be important in causing BaO ($A\,^1\Sigma^+$) M changes. Limiting ourselves to permanent BaO ($A\,^1\Sigma^+$) dipole and quadrupole moments (μ and Q, respectively), induced dipoles in Ar or CO_2 and the permanent quadrupole of CO_2, these interactions and corresponding BaO ($A\,^1\Sigma^+$) selection rules are: (i) dipole (BaO) ~ induced dipole (Ar or CO_2), $\Delta J = 0, \pm 2$, $\Delta M = 0, \pm 1, \pm 2$; (ii) dipole (BaO) ~ quadrupole (CO_2), $\Delta J = \pm 1$, $\Delta M = 0, \pm 1$; (iii) quadrupole (BaO) ~ induced dipole (Ar or CO_2), $\Delta J = \pm 1, \pm 3$, $\Delta M = 0, \pm 1, \pm 2, \pm 3$, and (iv) quadrupole (BaO) ~ quadrupole (CO_2), $\Delta J = 0, \pm 2$, $\Delta M = 0, \pm 2$.[5] Even assuming that these interactions were solely responsible for effecting J, M changes, more extensive changes in J, M occur via higher order terms involving the above operators; and, the selection rules above would not be rigorous. It seems reasonable that the interactions cited above would dominate small J, M changes. If so, dipole ~ induced dipole and quadrupole ~ quadrupole interactions could be expected to dominate elastic ($\Delta J = 0$) M changes; dipole ~ quadrupole and quadrupole ~ induced dipole interactions would dominate inelastic, odd $|\Delta J|$ M changes.

In this context, it is most interesting to compare our results to those of Borkenhagen *et al.* on CsF ~ rare gas M-changing collisions.[13] As mentioned above (Sec. I), cross sections of ~5 Å^2 were determined for elastic $(J, M) = (1, 0) \rightarrow (1, 1)$ transfer for CsF. By contrast, the BaO ($A\,^1\Sigma^+$) ~ Ar elastic cross section is no greater than 1 Å^2. The quadrupole moment for CsF ($X\,^1\Sigma^+$) is -2.0×10^{-25} esu cm^2. Although quadrupole moments have been determined for neither BaO ($X\,^1\Sigma^+$) nor $A\,^1\Sigma^+$, it is plausible that the $A\,^1\Sigma^+$ moment is significantly smaller than the $X\,^1\Sigma^+$ or CsF ($X\,^1\Sigma^+$) moments, since this state is more covalent (less polar) than either BaO ($X\,^1\Sigma^+$) or CsF ($X\,^1\Sigma^+$).[15,16] The charge distributions in the BaO and CsF ground states are probably similar in light of their nearly identical dipole moments and isoelectronic configurations.[16,28] However, the $A\,^1\Sigma^+ \leftarrow X\,^1\Sigma^+$ transition entails a partial charge transfer from $O(2p)$ to Ba($6s$) which not only reduces the dipole moment but also the quadrupole moment in $A\,^1\Sigma^+$ relative to $X\,^1\Sigma^+$. Thus, both first-order quadrupole and dipole ~ induced dipole interactions between BaO ($A\,^1\Sigma^+$) and Ar should be substantially weaker than the corresponding interactions between CsF ($X\,^1\Sigma^+$) and Ar, consistent with the elastic M-changing cross sections measured here and in Ref. 13.

It is interesting to note the important role which the CO_2 quadrupole moment -4.3×10^{-26} esu cm^2 plays in effecting $\Delta J = 0$, $\Delta M = 1$ transfer.[16] This moment may compensate for the small BaO ($A\,^1\Sigma^+$) dipole and quadrupole moments in causing $\Delta J = 0$, $\Delta M = 1$ transfer: the cross section for CO_2 collisions, into $M = \pm 1$, is 4.2 ± 1.2 Å^2 as mentioned above (Sec. III A), which is comparable to the CsF ~ rare gas values.[13]

Comparisons between CsF ($X\,^1\Sigma^+$) and BaO ($A\,^1\Sigma^+$) for inelastic transfer are more difficult since we have not determined individual $(J = 1, M) \rightarrow (J_f = 2, M_f)$ cross sections and Borkenhagen *et al.*[13] have determined only some of these cross sections. For rare gas collisions, Borkenhagen *et al.* observe equal branching into $M = 0$ or ± 1 for $J = 1 \rightarrow J_f = 2$, with cross sections of ≈ 4 Å^2.[16] If we assume the same branching ratio here and neglect population of $M = \pm 2$, the ratio of $I_\perp$ to $I_\parallel$ [Eq. (6)] would be 0.41, compared to an experimental value of 0.58 ± 0.05. The cross section into any particular M sublevel, 0 or ± 1, would be ≈ 6.7 Å^2 assuming a total $\Delta J = 1$ cross section of 20 Å^2.[1(a)] The value of $I_\perp/I_\parallel = 0.41$, calculated assuming identical branching to that found for CsF,[13] is qualitatively in accord with our experimental value (0.58).

TABLE II. Inelastic transition amplitudes $f'_{|m_1|\to|m_2|}$ for $J=1\to 2$ transfer in the c.m. system, quantized along the relative velocity vector. Amplitudes are calculated for atom–diatom collisions in the l-dominant approximation.[a] Relative values are given.[b]

$\lvert m_1\rvert$	$\lvert m_2\rvert$ = 2	1	0
1	1.25	2.50	3.06
0	1.77	3.50	4.30

[a]References 31 and 34.
[b]Absolute values depend on the total $J=1\to J_f=2$ transition amplitude. $j=80$.

2. Transformation to a center of mass system

We have been considering collision induced changes in the orientation of J with respect to a laboratory-fixed $\hat{z}$ axis specified by the direction of pump laser polarization. There are compelling reasons to transform to a center of mass (c.m.) system whose orientation is specified by the individual collision. All theoretical calculations do this and if useful M-changing generalizations are to emerge, they are likely to refer to such systems. We thus choose a quantization axis in the direction of the initial relative velocity vector, $\mathbf{v}_{rel}$.[29] Both initial (m_1) and final (m_2) projection quantum numbers are referred to this axis.

Let R be the required transformation operator and f an operator whose matrix elements give the amplitudes for sublevel to sublevel transitions in the c.m. system. The overall result of an inelastic ($\Delta J=\pm 1$) collision of $|10\rangle_{lab}$ BaO can then be represented by

$$\mathbf{R}^{-1}\mathbf{f}\,\mathbf{R}\,|10\rangle_{lab}=\sum_{M_f} a_{M_f}|2M_f\rangle_{lab}\,, \tag{8}$$

where M_f is the final projection quantum number along the *laboratory* fixed $\hat{z}$ axis and the a_{M_f} are final $J=2$ sublevel amplitudes. These amplitudes depend on the orientation (θ, ϕ) of $\mathbf{v}_{rel}$ with respect to the laboratory-fixed $\hat{z}$ axis; velocity averaging is required. The transformation procedure and velocity averaging is outlined elsewhere[30,31] and is treated in the Appendix here.

A model for the f matrix is needed to compute final sublevel amplitudes and populations. A full quantum treatment of atom-diatom ($^1\Sigma^+$) collisions[32] yields complicated expressions for f elements. Only in simple cases and with great computational effort can these expressions be evaluated. Therefore a number of approximations in limiting cases have recently been developed. We turn to some of these in order to calculate final sublevel populations for comparison with the polarization observed to be transferred to $J_f=2$ from $J=1$ by Ar collisions. (We observe the same polarization whether the collision partner is Ar or CO_2, but the quantum approximations we use are not expected to hold for the BaO $\sim CO_2$ case.)

3. The l-dominant approximation

This approximation, developed by DePristo and Alexander,[33,34] applies best when the dominant contributions to the scattering amplitude are from channels with large total angular momentum j.[35] This is so when the transition is principally the result of long-range encounters. Then, for a given j, channels with smallest orbital angular momentum l dominate because these channels have the lowest centrifugal barriers and smallest classical turning points. The l-dominant approximation in its simplest form neglects all channels (for a given j) except those with the smallest initial and final values of l.

The scattering amplitudes $f(\chi)_{J,m_1\to J,m_2}$ depend on scattering angle, χ (see Appendix). When they are evaluated in the l-dominant limit and $l\gg J$, these amplitudes factor into a product of a j, l independent term, f', and a summation over the j and l dependent terms. In this limit, the f' solely determine the branching, or relative amplitudes, into different M sublevels for a given $J\to J_f$ rotation changing collision. For $J=1\to J_f=2$, the different f' amplitudes are given in Table II. Additional details are given in the Appendix.

From Table II it is seen that the amplitudes are greatest when J is initially perpendicular to $\mathbf{v}_{rel}$, that is when $m_1=0$. In addition, the collision tends to align J perpendicular to $\mathbf{v}_{rel}$ for arbitrary initial orientation, that is $m_2=0$ transition amplitudes are largest.

Once c.m. f elements are known, final laboratory-fixed transition amplitudes, a_{M_f}, are obtained from Eq. (8). These a_{M_f} are differential scattering amplitudes, which still depend upon the orientation of $\mathbf{v}_{rel}$ with respect to space-fixed coordinates. To obtain integral transition probabilities in the laboratory system, $|a_{M_f}|^2$ are first averaged over all scattering angles and then averaged over all orientations of $\mathbf{v}_{rel}$. Details are given in the Appendix. The results are given in Table III.

The l-dominant approximation predicts high polarization transfer in the c.m. system, but the transfer is diminished in the laboratory-fixed system due to the coordinate transformations and velocity averaging. In fact, the calculated degree of polarization is slightly less than what is observed (Table III). This is expected from neglect of velocity selection by the pump laser (see Appendix).[36,37] We now turn to other prescriptions for the f elements to see how the agreement with observation is affected.

4. m conservation and the CS approximation

Greater polarization in the c.m. system is expected to lead, after velocity averaging, to greater polarization transfer in the laboratory-fixed system. Thus it is natural to next consider m conservation in the c.m. system. It should be noted that this selection rule is not physically meaningful in that it could lead to production of alignment when none initially existed in a system with no unique collision axis.[38] However, this model is useful in assessing the effect of such $\Delta m=0$ collisions apart from $\Delta m\neq 0$ collisions.

m conservation with respect to $\mathbf{v}_{rel}$ also arises when the centrifugal sudden (CS) or coupled states approximation is made to solve the close coupled equations.[39] This approximation decouples the orbital angular mo-

TABLE III. Inelastic transition probabilities $\overline{|a_{M_f}|^2}$, intensity ratios, and angles of rotation for $|1,0\rangle \rightarrow |2,M_f\rangle$ collisional transfer in $A\,^1\Sigma^+$ BaO.[a]

	$\overline{\lvert a_{M_f}\rvert^2}$					
$\lvert M_f\rvert$ =	0	1	2	$I_\perp/I_\parallel$	P	β
experiment	...	...	...	0.58 (5)	0.27 (5)	36° (1)
l dominant	0.26	0.23	0.14	0.70	0.18	42°
$\Delta m = 0$	0.40	0.30	0.00	0.37	0.46	28°
$\lvert\Delta m\rvert = 1$	0.50	0.22	0.03	0.35	0.48	27°

[a]Averaged over scattering angles and orientations of initial relative velocity vector. See text for definitions. 1σ errors in the last digit are given in parentheses.

mentum of the collision complex (1) from the diatom angular momentum, replacing it by a constant. If this constant is chosen to be the final value of the orbital angular momentum (l_f), scattering amplitudes vanish unless they conserve m.[40]

This m conserving rule has been applied by others to interpret the results of rotational energy transfer experiments.[41] When it is used in Eqs. (8) and (A4) and averaging over scattering angle and initial relative velocities performed as above, we obtain an intensity ratio of 0.37 ($P = 0.53$ and $\beta = 28°$). The predicted $J = 2$ polarization is now, as expected, greater than in the l-dominant approximation and also greater than is experimentally observed; the angle of rotation β is smaller.

5. $\Delta m = \pm 1$ selection rules

Another simple prescription is $\Delta m = \pm 1$; that is all elements with $|m_2 - m_1| = 1$ are equal and all others vanish. J, if initially perpendicular to $\mathbf{v}_{rel}$, is tipped by the collision toward $\mathbf{v}_{rel}$. This contrasts with the l-dominant atom–diatom limit where the collision aligns J perpendicular to $\mathbf{v}_{rel}$. When this prescription for f is used in Eq. (8) and the transformations carried out, the M_f populations and corresponding intensity ratio are surprisingly similar to the $\Delta m = 0$ case (Table III).

The m-conserving and $\Delta m = \pm 1$ models both predict greater $J = 2$ polarization than is observed; the difference from our experimental result may in part be accounted for by molecules that enter the state after more than one collision. High conservation of polarization in the c.m. system is compatible with observation, but the l-dominant amplitudes lead to slightly better agreement with observation than do these simple prescriptions. We observe the same $J = 2$ polarization whether Ar or CO_2 is the collision partner. The calculations show, however, that the same laboratory-fixed polarization can be consistent with different c.m. selection rules; thus the f elements for collisions with CO_2 may differ from those for Ar collisions yet yield the same observed polarization.

IV. CONCLUSIONS

Optical–optical double resonance spectroscopy, with its high resolution and selectivity, is well-suited for the investigation of elastic and inelastic M-changing collisions. At low J, with proper choice of laser and detection polarizations, direct measurement of M sublevel populations is possible. The extent of polarization transfer by collisions can be characterized and rules governing M changes determined.

Here, simplified experiments with $A\,^1\Sigma^+$ BaO, excited to $J = 1$, $M = 0$, show the power of the technique. Elastic M-changing collision cross sections are found to scale, at least qualitatively, with the diatom multipole moments, indicating the importance of long-range interactions in effecting molecular depolarization.

In modeling inelastic M-changing collisions, we have found the l-dominant theory of DePristo and Alexander[33,34] to be in accord with experiment. This again illustrates the dominance of long-range, large-impact parameter collisions in causing changes in magnetic sublevels and destruction of alignment.

These are first results demonstrating the potential of the method. Insight is gained into the way collisions change M quantum numbers and reorient molecules. Further work at low J under single-collision conditions and with other polarization configurations can provide more complete information on collisionally created M sublevel populations and M-changing rules.

ACKNOWLEDGMENTS

We are grateful to M. Alexander, J. Kinsey, and D. Pritchard for helpful discussions. This work was supported, in part, by grants from the Research Corporation (to SJS) and the National Science Foundation (CHE 75-05959, 75-19410, and 78-18427).

APPENDIX: CALCULATION OF SPACE-FIXED INELASTIC TRANSITION PROBABILITIES USING CENTER OF MASS TRANSITION AMPLITUDES

The pump laser prepares $|1,0\rangle$, quantized along space-fixed $\hat{z}$. Transformation to a center of mass (c.m.) system with quantization in the initial velocity, $\mathbf{v}_{rel}$, direction is effected by the D^1 rotation matrix[42]:

$$R\,|10\rangle = \sum_m D^{1*}_{0m}(\theta,\phi)\,|1m\rangle\,, \tag{A1}$$

where m is the c.m. projection quantum number, θ and ϕ specify the orientation of $\mathbf{v}_{rel}$ with respect to $\hat{z}$, and

* denotes complex conjugate. If $f_{1m_1\to 2m_2}(j, l, \mathbf{R})$ is the amplitude for the $|1, m_1\rangle \to |2, m_2\rangle$ transition, the result of inelastic transfer to $J=2$ is

$$fR|10\rangle = \sum_{m_1, m_2} D^{1*}_{0m_1} f_{1m_1\to 2m_2}(\chi)|2m_2\rangle \equiv \sum_{m_2} C_{m_2}|2m_2\rangle , \quad \text{(A2)}$$

where $C_{m_2} = \sum_{m_1} D^{1*}_{0m_1} f_{1m_1\to 2m_2}(\chi)$ is the amplitude for transfer to the c.m. quantized level $|2m_2\rangle$. To obtain space-fixed amplitudes, axis rotation back to the $\hat{z}$ direction is required:

$$R^{-1}fR|10\rangle = \sum_{m_2} R^{-1}C_{m_2}|2m_2\rangle \equiv \sum_{m_2, M_f} D^2_{M_f m_2}(\theta, \phi) C_{m_2}|2M_f\rangle \equiv \sum_{M_f} a_{M_f}|2M_f\rangle , \quad \text{(A3)}$$

where $a_M = \sum_{m_2} C_{m_2} D^2_{M_f m_2}(\theta, \phi)$ is the amplitude for transfer to the space-fixed level $|2, M_f\rangle$. The probabilities for collisional transfer into different M_f levels are then $|a_{M_f}|^2$; they depend on θ but not on ϕ since there is symmetry about $\hat{z}$.

In the fully quantum treatment the c.m. transition amplitudes are given by

$$f_{J_1 m_1\to J_2 m_2}(\chi) = \sum_{j=0}^{\infty} \sum_{l_1=|j-J_1|}^{j+J_1} \sum_{l_2=|j-J_2|}^{j+J_2} i^{l_2-l_1}\pi^{1/2}(-1)^{J_1+J_2}(2j+1)(2l_1+1)^{1/2} \times \begin{pmatrix} J_1 & l_1 & j \\ m_1 & 0 & -m_1 \end{pmatrix} \begin{pmatrix} J_2 & l_2 & j \\ m_2 & m_1-m_2 & -m_1 \end{pmatrix} T^j_{J_1 l_1, J_2 l_2}(\chi) Y_{l_2 m_1 - m_2}(\hat{R}) , \quad \text{(A4)}$$

where l_1 and l_2 are the initial and final angular momenta, respectively, Y_{lm} is a spherical harmonic, $T_{J_1 l_1, J_2 l_2}$ is a transition matrix element independent of m_1 or m_2, $\hat{R}$ denotes orientation of the vector joining the atom with the diatom c.m. and χ is the c.m. scattering angle.[31,32]

In the l-dominant limit, l_1 and l_2 are restricted to $j-J_1$ and $j-J_2$, respectively, and only the summation over j remains in Eq. (A4).[34] If we consider only those cases where $j \gg J_1$ and J_2, since the major contribution to the integral cross sections results from large values of j, the 3-j symbols in Eq. (A4) approach their asymptotic limits and vary as $j^{-1/2}$.[34,39] Thus the J_1, m_1, J_2, m_2 dependent factors in Eq. (A4) are approximately independent of j, l_1, and l_2 and can be factored out of the summation over j[34]:

$$f_{J_1 m_1\to J_2 m_2}(\chi) \sim f'_{J_1 m_1\to J_2 m_2} \sum_{j=0}^{\infty} F(j, \chi) Y_{l_2 m_1 - m_2}(\hat{R}) , \quad \text{(A5)}$$

where $F(j, \chi)$ includes the T matrix elements and other j, χ dependent terms. The f factors for $J_1=1$ and $J_2=2$ are given in Table II; these were computed assuming $j=80$, which is sufficiently large for Eq. (A5) to be valid.

When probabilities, $|a_{M_f}|^2$, are calculated and averaged over $\hat{R}$ and χ, the following expressions are obtained *in the l-dominant approximation*:

$$\overline{|a_0|^2} \sim (3/4^4)(5x^6 + 3x^4 + 3x^2 + 5) ,$$
$$\overline{|a_1|^2} \sim (1/2^7)(-5x^6 + 9x^4 + 5x^2 + 7) , \quad \text{(A6)}$$
$$\overline{|a_2|^2} \sim (1/2^9)(5x^6 - 45x^4 + 35x^2 + 21) ,$$

where $x = \cos\theta$ and M_f-independent terms have been supressed. The relative probabilities for transfer from $(J, M) = (1, 0)$ to $(J_f = 2, M_f)$ given in Eq. (A6) need only be averaged over θ, the orientation of $\mathbf{v}_{rel}$ relative to the space-fixed $\hat{z}$ axis.[43]

Averaging over initial relative velocities can be simply done if the BaO velocity selection by the pump laser is ignored.[36,37] In this case all directions are equally probable and the speed distribution is Maxwellian. In this case

$$\overline{x^{2n}} = \frac{\int_0^{\pi} \cos^{2n}\theta \sin\theta\, d\theta}{\int_0^{\pi} \sin\theta\, d\theta} = \frac{1}{2n+1} . \quad \text{(A7)}$$

The resultant velocity averaged relative probabilities $\overline{|a_{M_f}|^2}$ are given in Table III.

When other prescriptions for the scattering amplitudes are used, Eq. (A4) still applies. If we impose $\Delta m = 0$ or ± 1 selection rules, an equation analogous to Eq. (A5) results: the m dependence can be factored out and branching ratios into different m sublevels obtained. For m conservation,

$$f'_{1m_1\to 2m_2} = \delta_{m_1 m_2} \quad \text{(A8)}$$

and for $\Delta m = \pm 1$ selection rules,

$$f'_{1m_1\to 2m_2} = \delta_{|m|1} , \quad \text{(A9)}$$

where $m = m_1 - m_2$. Similar equations to Eq. (A6) are obtained and velocity averaged using Eq. (A7) to give the results in Table III.

[1](a) R. A. Gottscho, S. J. Silvers, R. Bacis, and R. W. Field, J. Chem. Phys. **73**, 599 (1980). (b) R. A. Gottscho, J. B. Koffend, R. W. Field, and J. R. Lombardi, J. Chem. Phys. **68**, 4110 (1978), and references therein. (c) R. A. Gottscho, Ph. D. thesis, M.I.T., 1979, and references therein.

[2]R. G. Gordon, J. Chem. Phys. **45**, 1643 (1966).

[3]R. B. Kurzel and J. I. Steinfeld, J. Chem. Phys. **56**, 5188 (1972).

[4](a) R. Clark and A. J. McCaffery, Mol. Phys. **35**, 617 (1978); (b) S. R. Jeyes, A. J. McCaffery, and M. D. Rowe, *ibid.* **36**, 845 (1978); (c) M. D. Rowe and A. J. McCaffery, Chem. Phys. **34**, 81 (1978); **43**, 35 (1979).

[5]T. Oka, Adv. At. Mol. Phys. **9**, 127 (1973).

[6]R. L. Shoemaker, S. Stenholm, and R. G. Brewer, Phys. Rev. A **10**, 2037 (1974).
[7]J. W. C. Johns, A. R. W. McKellar, T. Oka, and M. Romheld, J. Chem. Phys. **62**, 1488 (1975).
[8]Ph. Brechignac, A. Picard-Bersellini, and R. Charneau, J. Phys. B **13**, 135 (1980).
[9]S. J. Silvers and C. L. Chiu, J. Chem. Phys. **56**, 5663 (1972).
[10]E. M. Weinstock, R. N. Zare, and L. A. Melton, J. Chem. Phys. **55**, 1468 (1971).
[11]T. A. Caughey and D. R. Crosley, Chem. Phys. **20**, 467 (1977).
[12]J. R. R. Leite, M. Ducloy, A. Sanchez, D. Seligson, and M. S. Feld, Phys. Rev. Lett. **39**, 1465 (1977). These experiments create coupled three-level systems by tuning cross-polarized probe and saturating laser beams to the same transition. The probe signals are narrowed by the saturating field and their shapes depend, in part, on alignment relaxation rates. The rate of excited state alignment-decay can be extracted in the absence of external fields.
[13]V. Borkenhagen, H. Maithan, and J. P. Toennies, J. Chem. Phys. **71**, 1722 (1979).
[14]This result is not necessarily inconsistent with Kurzel and Steinfeld's result (Ref. 3) since $M = J\cos\alpha$, where α is the reorientation angle. For constant M, a change in J necessarily implies a change in α.
[15]R. F. Wormsbecher, S. L. Lane, and D. O. Harris, J. Chem. Phys. **66**, 2745 (1977).
[16]A. D. Buckingham, in *Physical Chemistry, Vol. IV, Molecular Properties*, edited by D. Henderson (Academic, New York, 1970), p. 349.
[17](a) C. R. Jones and H. P. Broida, J. Chem. Phys. **60**, 4369 (1974); (b) J. B. West, R. S. Bradford, Jr., J. D. Eversole, and C. R. Jones, Rev. Sci. Instrum. **46**, 164 (1975).
[18]The quantization axis, chosen along the pump polarization direction, is not parallel to the earth's magnetic field. It is possible for precession about the field to depolarize the prepared state. Assuming an A state g factor of $\sim 10^{-3}$, such precession amounts to only $\sim 10^{-4}$ Hz during the state's lifetime. Depolarization due to the earth's field can accordingly be neglected.
[19]K. Blum, in *Progress in Atomic Spectroscopy, Part A*, edited by W. Hanle and H. Kleinpoppen (Plenum, New York, 1979), p. 71.
[20]W. E. Baylis, in *Progress in Atomic Spectroscopy, Part B*, edited by W. Hanle and H. Kleinpoppen (Plenum, New York, 1979), p. 1227.
[21]A. Corney, *Atomic and Laser Spectroscopy* (Clarendon, New York, 1977).
[22]Throughout this paper, we use J'' and J^* to refer to $X\,^1\Sigma^+$ and $C\,^1\Sigma^+$ rotational levels, rsspectively. J and J_f refer to $A\,^1\Sigma^+$ levels prepared initially by the pump laser and populated subsequently by collisions, respectively. Generally, magnetic quantum numbers are referred to space-fixed axes except where explicitly stated that a center of mass reference system is being employed.
[23]J. T. Hougen, Natl. Bur. Stand. U.S. Mono. 115 (1970).
[24]At the lower pressures of 0.3 Torr Ar and 0.03 Torr CO_2, assuming from Ref. 1(a) total rotationally inelastic cross sections of 50 Å^2 for BaO ~ Ar and BaO ~ CO_2 collisions, respectively, an excited BaO molecule undergoes on the average 0.6 rotational transitions within its lifetime.
[25]S. E. Johnson, J. Chem. Phys. **56**, 149 (1972).
[26]When the CO_2 and Ar pressures are similar, BaO molecules reach $J = 2$ principally through collisions with CO_2; the $\Delta J = 1$ cross sections for CO_2 collisions are as much as ten times greater than those for Ar (Ref. 1a). In some experiments, however, the Ar pressure is 10^2 times greater than the CO_2 pressure. Then it is likely that most molecules reach $J = 2$ through Ar collisions. If depolarization with Ar differed significantly from that with CO_2, the $I_\perp/I_\parallel$ ratio would not be the same in these two cases.
[27]The rotation is taken about $\hat{y}$ and the rotated state expressed in terms of unrotated M sublevels using the rotation matrix $D^2_{M',M}(0,\beta,0)$. The squares of the sublevel amplitudes are used as population densities (n_i) in Eq. 6 and $I_\perp/I_\parallel$ obtained as a function of β. The observed intensity ratio then implies $\beta = 36°$.
[28](a) L. Wharton, M. Kaufman, and W. Klemperer, J. Chem. Phys. **37**, 621 (1962); (b) L. Wharton and W. Klemperer, *ibid.* **38**, 2705 (1963).
[29]Other choices are possible, such as quantization along the final relative velocity vector. For a discussion of such choices see V. Khare, D. J. Kouri, and R. T Pack, J. Chem. Phys. **69**, 4419 (1978).
[30]J. L. Kinsey, J. W. Riehl, and J. S. Waugh, J. Chem. Phys. **49**, 5269 (1968).
[31]M. H. Alexander, P. J. Dagdigian, and A. E. DePristo, J. Chem. Phys. **66**, 59 (1977).
[32](a) A. M. Arthurs and A. Dalgarno, Proc. R. Soc. London Sect. A **256**, 540 (1960); (b) D. Secrest, in *Atom-Molecule Collision Theory*, edited by R. B. Bernstein (Plenum, New York, 1979), p. 265.
[33](a) A. E. DePristo and M. H. Alexander, J. Chem. Phys. **63**, 3552, 5327 (1975); **64**, 3009 (1976); **66**, 1334 (1977); (b) A. E. DePristo and M. H. Alexander, J. Phys. B **9**, 2713 (1976).
[34]M. H. Alexander and P. J. Dagdigian, J. Chem. Phys. **66**, 4126 (1977).
[35]The total angular momentum of the atom-diatom ($^1\Sigma^+$) system is the sum of the orbital angular momentum associated with relative atom–diatom motion (l) and rotational angular momentum of the diatom (J).
[36]Since the BaO mass is approximately four times that of Ar or CO_2, this assumption is not very restrictive. For example, the root mean square relative speed along $\hat{x}$, the laser propagation direction, is 4.3×10^4 cm sec^{-1} without velocity selection and 3.8×10^4 cm sec^{-1} with velocity selection. Neglect of velocity selection will yield upper bounds to depolarization since velocity selection tends to caus polarization alignment and orientation.[41]
[37]M. Elbel, H. Hühnermann, Th. Meier, and W. B. Schneider, Z. Physik, A **275**, 339 (1975); M. Elbel (private communication).
[38]For example, if the initial state were the spherically symmetric scale $J = 0$, $m = 0$ and the final state were $J \neq 0$, $m = 0$, alignment would have been created even if there is no velocity selection. This is impossible. The selection rules on m changes are actually dictated by the 3-j symbols in Eq. (A4).
[39](a) P. McGuire and D. J. Kouri, J. Chem. Phys. **60**, 2488 (1974); (b) V. Khare, D. J. Kouri, and R. T Pack, J. Chem. Phys. **69**, 4419 (1978); (c) D. J. Kouri, in *Atom-Molecule Collision Theory*, edited by R. B. Bernstein (Plenum, New York, 1979), p. 301.
[40]Other choices are discussed in Ref. 39(b). For example, if the initial value of l is used, the projection of diatom angular momentum along the final relative velocity vector is conserved.
[41](a) T. A. Brunner, R. D. Driver, N. Smith, and D. E. Pritchard, Phys. Rev. Lett. **41**, 856 (1978); (b) T. A. Brunner, R. D. Driver, N. Smith, and D. E. Pritchard, J. Chem. Phys. **70**, 4155 (1979).
[42]M. E. Rose, *Elementary Theory of Angular Momentum* (Wiley, New York, 1957).
[43]To be correct, the differential transition probabilities should be converted to rate constants and then number densities before averaging over scattering angles and initial velocities. We have neglected the dependence of transition probabilities on relative kinetic energy.